

Molecular Dynamics Study on the Glass Transition in $\text{Ca}_{0.4}\text{K}_{0.6}(\text{NO}_3)_{1.4}$ Mauro C. C. Ribeiro[†]*Laboratório de Espectroscopia Molecular, Instituto de Química, Universidade de São Paulo C.P. 26077, CEP 05513-970, São Paulo, SP, Brazil**Received: March 5, 2003; In Final Form: May 29, 2003*

Molecular dynamics (MD) simulations of the glass-forming liquid $\text{Ca}_{0.4}\text{K}_{0.6}(\text{NO}_3)_{1.4}$ (CKN) have been performed at several temperatures from a liquid state at 800 K down to a glassy state at 150 K. The well-known Ewald summation method of handling the long-range electrostatic interactions has been replaced by the recently proposed method of truncated shifted Coulomb potential (Wolf; et al. *J. Chem. Phys.* **1999**, *10*, 8254). Some comparisons between dynamical properties of liquid CKN simulated with either of these methods are provided. A previously introduced polarizable fluctuating charge model (FCM) for the nitrate anion (Ribeiro, M. C. C. *Phys. Rev. B* **2000**, *61*, 3297) has been used. It is shown that the FCM is an improvement on the nonpolarizable rigid ion model (RIM) counterpart as the glass transition temperature T_g of the system simulated with the FCM is in better agreement with the experimental calorimetric value ($T_g \approx 475$, 380, and 335 K for the RIM, FCM, and experiment, respectively). Reorientational time correlation functions, $P_2(t)$, are first analyzed as in previous Raman spectroscopy investigations (Jacobsson; et al. *J. Non-Cryst. Solids* **1994**, *172–174*, 161), where the reorientational relaxation time, τ_{or} , was obtained from the short time decay of $P_2(t)$. Excellent agreement between experimental and calculated τ_{or} has been found, including the Arrhenius dependence of τ_{or} across T_g . It is shown, however, that the above analysis of the experimental $P_2(t)$, where only the short time decay is available, is misleading. Contrary to the Raman results, a marked change in activation energy across T_g is obtained when the long time decay of the calculated $P_2(t)$ is considered. The temperature dependence of τ_{or} is further compared with the diffusion coefficient, D , and the structural α -relaxation time, τ_α , obtained from the self-part of the intermediate scattering function. The hierarchy of the decoupling between τ_{or} , D , and τ_α as CKN is cooled to T_g is shown.

I. Introduction

Molecular dynamics (MD) simulations have played a fundamental role in our understanding of the dramatic dynamical changes that supercooled liquids undergo on approaching the glass transition temperature, T_g . Despite intrinsic limitations on time and spatial ranges that can be probed by MD simulations, many issues on the dynamics of glass-forming liquids have been addressed, such as structural and dynamical heterogeneity, the temperature dependence of the diffusion coefficient and the structural relaxation, the role played by activated hopping processes as the liquid is cooled to T_g , etc.^{1,2} To achieve feasible simulation runs, many of these simulations have been devoted to simple models, such as binary mixtures of atomic Lennard-Jones systems whose potential parameters are appropriate to prevent crystallization.³ Certainly, MD simulations of realistic models, for instance, SiO_2 ,⁴ are also needed for direct comparison to actual experimental data, and indeed, previous MD simulations of more complex models of molecular glass-forming liquids, such as *o*-terphenyl⁵ and ethanol,⁶ have been reported.

In this work, we are concerned with the dynamics of the well-known glass-forming liquid CKN, $\text{Ca}_{0.4}\text{K}_{0.6}(\text{NO}_3)_{1.4}$. CKN is an archetypical fragile glass-forming liquid, i.e., a glass-forming liquid whose viscosity increases under cooling in a non-Arrhenius fashion at temperatures close to T_g .^{7,8} Structure and dynamics of CKN have been the subject of several spectroscopic investigations.^{9–13} A previous MD simulation of CKN has been reported by Signorini et al.,¹⁴ and more recently, their model (a

nonpolarizable rigid ion model, RIM) has been modified to include polarization effects in a fluctuating charge model, FCM.^{15–18} The most important difference between the FCM and the original RIM for CKN is that the so-called pre-peak in the calculated static structure factor, $S(k)$, which is an indication of an intermediate-range order, was observed as in the experimental $S(k)$ provided that polarization effects were included in the simulations.^{10,15} Concerning the dynamics, polarization effects increase the diffusion coefficients and the rate of structural relaxation of the simulated system.¹⁷ This finding also points to a general improvement of the FCM on the previous RIM,¹⁴ because it was recognized that the RIM was a too stiff model as the ionic mobilities seemed to cease in a temperature range higher than the experimental T_g .

The first aim of the present work is to provide more direct evidence that T_g of CKN simulated with the FCM is indeed closer to the experimental T_g than the one obtained with the RIM. In MD simulations, T_g is usually estimated by calculating the equilibrium density of the system with decreasing temperature and identifying the change of the slope in a density vs temperature plot. On a technical perspective, the present MD simulations have been performed by using the recently proposed method of Wolf et al.¹⁹ for handling the long-range electrostatic interactions. The Wolf method is particularly appealing for the present application because long MD runs at many different temperatures are needed. The Wolf method is based on a truncated shifted Coulomb potential, which is computationally faster than the well-known Ewald sum method.²⁰ As the Wolf method has been used previously only in a few systems,^{19,21,22}

[†] E-mail: mccribe@quim.iq.usp.br.

and the Ewald sum method is certainly a reference procedure of handling long-range interactions in ionic systems, we provide some comparisons between results of liquid CKN simulated with either of these methods.

The second aim of the present work is to compare the reorientational, translational, and structural relaxation of CKN across the glass transition. Being confident that the dynamics of CKN simulated with the FCM is more representative of the real system than the RIM, we then investigate the temperature dependence of relaxation times obtained with the FCM from a high-temperature liquid state at 800 K down to a glassy state at 150 K. In a previous Raman spectroscopy investigation of CKN in a comparable large temperature range,¹¹ it has been found that the reorientational relaxation time, τ_{or} , follows an Arrhenius dependence with no sign of change in the activation energy across T_g .¹³ On the other hand, NMR spectroscopy studies on CKN indicated a sharp change on the relaxation time at T_g . It will be shown that the present MD simulations agree with the Raman results as long as the calculated reorientational time correlation functions, $P_2(t)$, are analyzed in the same way as the experimental ones, that is, by taking into account only the short time ($t < 1.2$ ps) decay. However, that is misleading, as a change in activation energy actually occurs at T_g when the long time behavior of $P_2(t)$ is considered. The temperature dependence of reorientational relaxation given by τ_{or} is further compared with the translational diffusion coefficient, D , and the structural relaxation time, τ_{α} . Decoupling between reorientational, translational and structural relaxation occurs as CKN is cooled to the glassy state. Such a decoupling comes from hopping processes that allow single-particle motions despite a freezing structure. Similar findings have been also observed in atomic systems,³ and the present case of CKN opens the possibility of further showing a decoupling between reorientational and translational dynamics.

The paper is organized as follows. Computational details are given in section II. As the FCM for CKN has been introduced in previous publications,^{15–18} it is presented here briefly. Comparisons between some properties of liquid CKN simulated with either the Wolf method or the Ewald sum method of handling the long-range interactions are given. In section III, the results and discussion are presented in three subsections. We first compare T_g estimated with either the FCM or its nonpolarizable RIM counterpart with the experimental T_g . Then, reorientational time correlation functions calculated with the FCM are analyzed in the same way as the previous Raman band shape studies by Jacobsson et al.,¹¹ that is, by using only the short time decay as available in the experiment. Finally, reorientational, translational and structural relaxation times of CKN are compared in a large temperature range. Concluding remarks are given in section IV.

II. Computational Details

In the fluctuating charge model (FCM) for CKN,¹⁵ polarization effects in the NO_3^- anion are included by allowing variable partial charges on the atoms in the anion, instead of the usual fixed partial charges scheme. The environment that an anion experiences in a given configuration of the system induces a charge flow between the atoms in the anion constrained by the total charge -1 . (Charge transfer is not allowed between different ions.) The magnitude of the charge transfer between the atoms in a given anion is dictated by the electronegativity equalization method (EEM).^{15,23,24} The EEM states that the electronegativities of the atoms in a given molecule are all equal at the equilibrium, where the electronegativity is the derivative

of the electrostatic energy that is given by a quadratic expansion in terms of the charges. The parameters of this expansion are the adjustable parameters of the model, which were obtained previously for the NO_3^- anion.^{15,16} The force that drives the partial charge of a given atom in an anion in the MD simulation is due to the departure of the instantaneous electronegativity of that atom from the average electronegativity of the anion. The partial charges are updated simultaneously with the ionic coordinates at each time step of the simulation; that is, the partial charges are additional degrees of freedom with their own equation of motion. The NO_3^- anion is considered as a rigid body, so that a quaternion approach is used to solve the rotational equations of motion.²⁰ The cations are nonpolarizable and carry their full charge.

The FCM for CKN has been built on a previous nonpolarizable rigid ion model (RIM),¹⁴ which considers a pairwise additive Born–Mayer potential. The parameters for the short-range and the polarizable parts of the potential can be found in previous publication.^{14–18} CKN has been simulated by considering 996 ions (166 Ca^{2+} , 249 K^+ , and 581 NO_3^-) in a cubic box with variable volume at fixed zero pressure. [In previous publications,^{15–18} we simulated a smaller system (501 ions) in a *NVE* ensemble.] Temperature and pressure have been controlled by using the scheme proposed by Berendsen et al.²⁵ of weak coupling of the system to a bath. CKN has been simulated from a high-temperature well-equilibrated liquid state at 800 K, down to a deep glassy state at 150 K. Temperature has been decreased in steps of 50 K, allowing for a typically 1.0 ns period at each temperature. (At low temperatures, the period at each temperature was extended to about 2.0 ns). The time step used in the simulations was 1.0 fs, which is dictated by the fast dynamics of the fluctuating charges. The whole process of cooling the system was repeated to confirm the calculated average densities. A third cooling procedure has been also done with no polarization effects by switching off the charge fluctuation, and using the values of the fixed partial charges of the original RIM.¹⁴

The whole protocol of cooling the system through the glass transition involves millions of steps of simulation. As mentioned in the Introduction, the present MD runs were made faster by using the method of handling the long-range electrostatic interactions proposed by Wolf et al.,¹⁹ instead of the well-known Ewald sum method.²⁰ In the Wolf method, the Coulombic interaction between two charges is evaluated as long as the distance between them is smaller than a chosen cut radius, R_c . A damping error function with an adjustable parameter α is considered. A key point in the method is to ensure charge neutrality in the spherical volume around a given charge, which has been demonstrated to be equivalent of using a shifted potential scheme. The practical advantage of the method is obvious, as the resulting truncated shifted Coulomb interactions are evaluated in the same foot as the short-range interactions. Demontis et al.²¹ gave a detailed analysis of the CPU time saving by using the Wolf method instead the Ewald sum method.

The Wolf method has been tested and compared with the Ewald sum method for few systems, for instance, NaCl ,¹⁹ MgO ,¹⁹ aluminosilicates,²¹ and water.²² It would be interesting to assess here whether the resulting dynamics of the simulated CKN suffers from artifacts due to the use of the Wolf method, keeping the well-established Ewald sum method as a reference simulation protocol. In this respect, we have done several MD runs of liquid CKN at 800 K to compare the methods. In addition, eventual effects on the dynamics of CKN due to the use of the Berendsen thermostat and barostat have been also

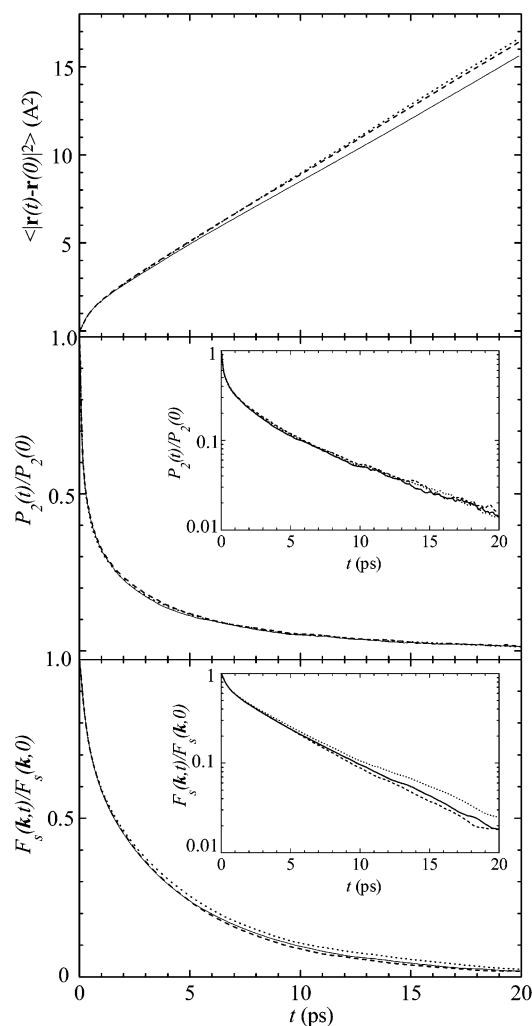


Figure 1. Mean square displacement, $\langle |\mathbf{r}_i(t) - \mathbf{r}_i(0)|^2 \rangle$, the reorientational time correlation function, $P_2(t)$, and the self-part of the intermediate scattering function, $F_s(\mathbf{k}, t)$, at $k = 1.46 \text{ \AA}^{-1}$, of the NO_3^- anions in CKN simulated with the FCM at 800 K. The full line is the result obtained with the Ewald sum method in a NVE ensemble, and the dashed line with the Wolf method with the Berendsen's thermostat and barostat switched on. The dotted line is the result with the Wolf method in a NVE ensemble. The insets show the data in a logarithm scale.

addressed, by running further MD simulations in a NVE ensemble at a fixed density corresponding to the average density previously determined.

A detailed analysis of the effects of changing the parameters in the Wolf method (α and R_c) has been reported recently for liquid water.²² The recommended values were $\alpha = 0.2 \text{ \AA}^{-1}$ and $R_c = 9.0 \text{ \AA}$, in the sense that thermodynamic averages, the structure, and the dynamics of the simulated system are comparable with the results obtained with the Ewald sum method. It has been shown that the average density of liquid water simulated with the Wolf method was dependent on the chosen cut radius for small R_c values, and R_c not smaller than 9.0 \AA has been suggested.²² A slight dependence of the average density on R_c has been also observed here in case of liquid CKN at 800 K. We considered $\alpha = 0.15 \text{ \AA}^{-1}$, and the calculated average density was 1.95 g/cm^3 when $R_c = 11.0 \text{ \AA}$, and 1.92 g/cm^3 when $R_c = 13.0 \text{ \AA}$. The last value seemed to be an appropriate compromise in the present case, as the same density was obtained with larger R_c . For comparison purposes, the size of the cubic box used in the present simulations ranged from 35.5 \AA at 800 K to 33.6 \AA at 150 K.

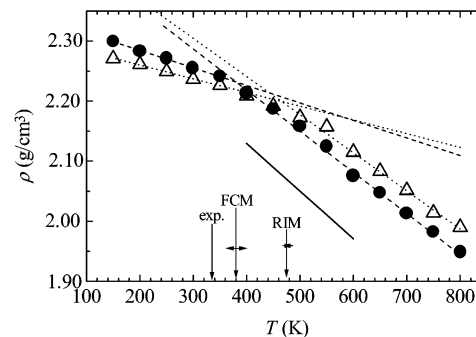


Figure 2. Calculated average densities of CKN simulated with the RIM (triangles) and the FCM (circles). The dashed lines are linear fits to the high- and low-temperature limits for either case. The bending in the slope in these plots gives the estimated glass transition temperature, T_g , as indicated by the vertical arrows, the experimental value also being given.²⁶ The small horizontal arrows give the uncertainty in the estimate T_g due to slightly different linear fits at high and low temperature. The full line is the experimental $\rho(T)$ curve for liquid CKN.²⁶

A detailed analysis of the equilibrium structure of liquid and glassy CKN has already been given in a previous publication.¹⁵ In this paper, we are concerned with the temperature dependence of the diffusion coefficient, D , the reorientational relaxation time, τ_{or} , and the structural α -relaxation time, τ_α , of CKN simulated with the FCM. Diffusion coefficients have been calculated from the slope at long time of the mean-square displacements, $\langle |\mathbf{r}_i(t) - \mathbf{r}_i(0)|^2 \rangle = 6Dt$, where $\mathbf{r}_i(t)$ is the coordinate of the center of mass of the ion i at time t . The reorientational time correlation function, $P_2(t)$, is given by

$$P_2(t) = \frac{1}{2} \langle 3[\mathbf{u}_i(t) \cdot \mathbf{u}_i(0)]^2 - 1 \rangle \quad (1)$$

where $\mathbf{u}_i(t)$ is a unitary vector on the C_3 axis of a given NO_3^- anion. Structural α -relaxation time has been obtained from the self-part of the intermediate scattering function, $F_s(\mathbf{k}, t)$:

$$F_s(\mathbf{k}, t) = \langle \exp\{i\mathbf{k}[\mathbf{r}_i(t) - \mathbf{r}_i(0)]\} \rangle \quad (2)$$

where \mathbf{k} is the wave vector.

Figure 1 shows a comparison between these time correlation functions in liquid CKN at 800 K simulated with three different simulation protocols at the same density. The results in Figure 1 indicate the agreement between dynamical properties obtained by using either the Wolf method or the Ewald sum method in liquid CKN. Furthermore, by comparing the results obtained with the Wolf method in a NVE ensemble and when the Berendsen thermostat and barostat are activated, one sees that the latter does not imply major perturbations on the dynamical properties of the simulated system. In summation, the Wolf method for handling the long-range electrostatic interactions in MD simulations of CKN gives results that compare well with the Ewald sum method. The greater computational efficiency of the former is a very interesting feature that makes it appropriate in long time MD simulations of ionic glass-forming liquids.

III. Results and Discussion

A. Identifying T_g in the Simulated Systems. Figure 2 shows plots of the average density vs temperature of liquid CKN simulated with the FCM and the RIM. The bending on the slope of these graphs indicates the glass transition temperature T_g . It is clear from Figure 2 that T_g calculated with the FCM is closer to the experimental value²⁶ than the RIM ($T_g \approx 475, 380$, and 335 K for the RIM, FCM, and experiment, respectively).

Experimental densities of liquid CKN in a limited temperature range (400–600 K) is also shown in Figure 2 according to the empirical equation $\rho \text{ (g}\cdot\text{cm}^{-3}) = (2.23 - 0.793) \times 10^{-3} T \text{ (}^\circ\text{C)}^{.26}$ The FCM results in average densities smaller than the RIM, but there still remains a systematic small departure of ca. 5.0% to the experimental data. On the other hand, it is interesting to note that the slope of the calculated $\rho(T)$ curve in the liquid phase agrees with the experimental one; that is, there is an agreement between simulated and experimental thermal expansion coefficient.

Determining T_g in MD simulations suffers from the unphysical large cooling rates proper to natural limitations on the time range accessible by the method. In fact, the dependence of the estimated T_g on the cooling rate has been the subject of recent MD simulations of simple atomic Lennard-Jones systems.^{27,28} It has been shown that faster cooling rates result in higher T_g . Most probably, the present estimated T_g of CKN could be made lower by using slower cooling rates. We stress that the comparison between the FCM and the RIM results shown in Figure 2 refers to the same cooling rate, so that a genuine model dependence on the calculated T_g is being addressed. Finally, the dynamics of supercooled liquids may be affected by finite size effects of the simulated systems, although the effects seems to be much weaker in fragile glass-formers.²⁹ In our previous MD simulations of CKN,^{15–18} we have considered 501 ions, and we have found here that it gives the same average densities as the present simulation of 996 ions.

In summation, we showed here that the previously reported¹⁷ increased ionic mobility in CKN due to polarization effects indeed results in the glass transition in a temperature range that is closer to the experimental calorimetric T_g . In other words, the RIM for CKN being a too stiff model, its dynamics in a given temperature actually corresponds to the real system dynamics at a lower temperature. Once we are confident that the dynamics of CKN simulated with the FCM is more representative of the real system than the RIM, in the following we discuss the dynamics of the FCM in the broad temperature range from liquid to glassy states.

B. Comparing Calculated τ_{or} with Raman Data. Raman band shape analysis has been used for several decades to reveal the dynamics of vibrational and reorientational relaxation in molecular and ionic liquids.^{30,31} A time correlation function can be obtained from a Raman spectrum by Fourier transforming any appropriate nonoverlapping Raman band. Depolarization measurements allow one to record the isotropic and the anisotropic Raman spectra, which result in the corresponding isotropic and anisotropic time correlation functions. The former is the vibrational time correlation function, whereas the latter has contribution from both the vibrational and the reorientational relaxation. Assuming that there is a time separation between these two processes, the pure reorientational time correlation function is obtained by the quotient between the anisotropic and the isotropic time correlation functions.

In the case of a Raman band of a totally symmetric normal mode of a symmetric top molecule, such as the NO_3^- anion, one probes the reorientation of a unitary vector on the main symmetry axis C_3 , i.e., a vector normal to the plane of the NO_3^- , as given by the single-particle $P_2(t)$ function, eq 1.³⁰ An important drawback of the Raman band shape analysis is that the time range and the time resolution of the time correlation functions are determined by the frequency resolution and the frequency window of the experimental Raman band. In a previous Raman band shape analysis of the totally symmetric ν_1 mode at 1050 cm^{-1} of the NO_3^- anion in CKN, $P_2(t)$ was

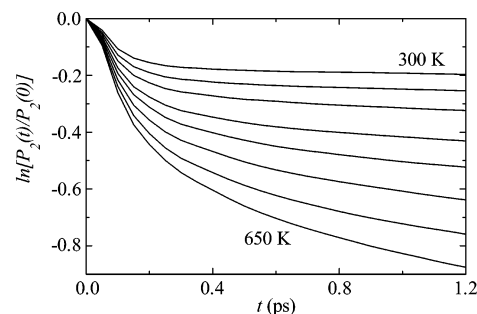


Figure 3. Short time range of the reorientational time correlation function of CKN simulated with the FCM. Each curve correspond to a 50 K interval from 650 to 300 K.

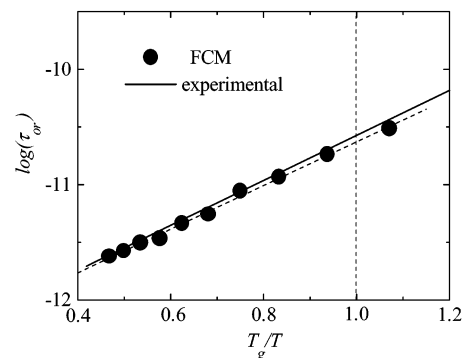


Figure 4. Reorientational relaxation time of CKN obtained from the short time range of the reorientational correlation function. The dashed line is a linear fit to the MD results, and the full line is the experimental data.¹¹

accessible in a limited time range (up to 1.2 ps).¹¹ Nevertheless, the reorientational relaxation time, τ_{or} , has been obtained by an exponential adjust of $P_2(t)$ for $t > 0.4$ ps. The most important conclusion in ref 11 was the Arrhenius dependence of τ_{or} , with no sign of any change in the activation energy across T_g . This is a rather important assertion because the coupling between reorientational and structural relaxation is a major issue in the context of glass-forming liquids, and of course, the structural relaxation time displays major changes on approaching T_g from above.

To compare the single-particle reorientational dynamics of the simulated CKN with the real system, we analyze the calculated $P_2(t)$ functions in the same way as in the previous Raman investigation. Figure 3 shows $P_2(t)$ of CKN simulated with the FCM at several temperatures, which compare well with the experimental data shown in Figure 2 of ref 11 in the same time window. By fitting an exponential function in the 0.4–1.2 ps range, one obtains corresponding relaxation time τ_{or} . Figure 4 shows the calculated τ_{or} in an Arrhenius plot (compare Figure 3 of ref 11), in which the temperature axis has been normalized by the T_g obtained in the previous section. It is clear from Figure 4 that the agreement between experimental and calculated τ_{or} is very good, in particular the finding of no change in activation energy across the glass transition.

Proper to the agreement between the MD simulations and the Raman spectra, Figure 4 is another indication that the dynamics of CKN is well represented by the FCM. Reorientational dynamics of CKN in a smaller temperature range (380–620 K) has been also investigated by transient optical Kerr effect,³² in which the time window extended up to ca. 40.0 ps. Although reorientational times were not obtained below T_g in ref 32, the obtained τ_{or} are of the same order of magnitude as the Raman data, and the observed temperature dependence of τ_{or} in the Kerr measurements is also in line with the Raman

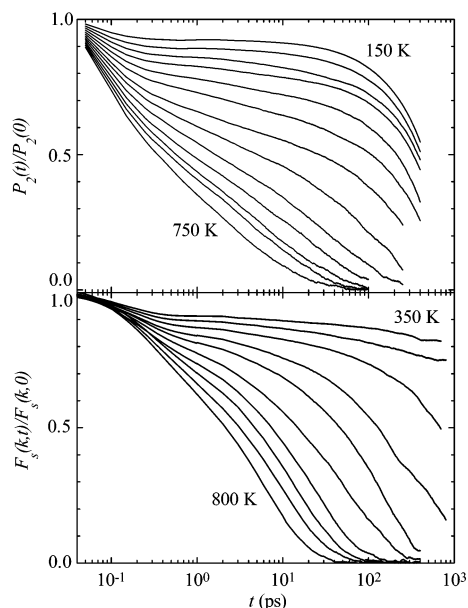


Figure 5. Reorientational time correlation function, $P_2(t)$, and the self-part of the intermediate scattering function, $F_s(\mathbf{k}, t)$, at $k = 1.46 \text{ \AA}^{-1}$, of the NO_3^- anions in CKN simulated with the FCM. Each curve corresponds to a 50 K interval from the high down to the low temperature indicated in the figure.

ones as no diverging behavior was found on approaching T_g . Thus, both the Raman and the Kerr measurements indicate the decoupling between reorientational and structural relaxation. A distinct finding observed in the Kerr results, however, is that one can identify a slight change in the slope of the temperature dependence of τ_{or} at $T \approx 430 \text{ K}$.³²

Actually, obtaining τ_{or} as in Figure 3 can be misleading, as it reflects only the initial decay of $P_2(t)$, that is, a time range that is too short for the particle to probe properly the structural relaxation. Thus, the continuous behavior of τ_{or} across T_g shown in Figure 4 indicates that no marked changes on the short-range structure and the short time dynamics occurs along the glass transition. Were one to consider the long time decay of $P_2(t)$, one would get a different picture of the reorientational dynamics in CKN across the glass transition. We stress that the analysis of $P_2(t)$ performed in this section was intended to demonstrate that the present MD simulations are consistent with the Raman data. A more faithful picture of the temperature dependence of the reorientational dynamics in CKN is derived when the long time decay of the simulated $P_2(t)$ is taking into account, what is shown in the next section together with the diffusion coefficient and the structural relaxation time.

C. Comparing Reorientational, Translational, and Structural Relaxation Dynamics. Figure 5 shows $P_2(t)$ and the self-part of the intermediate scattering function, $F_s(\mathbf{k}, t)$, of the NO_3^- anions at $k = 1.46 \text{ \AA}^{-1}$ (the main peak of the corresponding partial static structure factor)^{15,17} calculated with the FCM for CKN. These functions display the well-known two-step decay observed in glass-forming liquids, where an initial short-time decay is followed by a plateau at intermediate times and then a slow decay (α relaxation) which is stretched in time.^{1–6} The latter is very much dependent on temperature and slows down significantly on approaching T_g . The finding that the behavior of $P_2(t)$ closely follows the structural relaxation probed by $F_s(\mathbf{k}, t)$ implies that low-frequency Raman spectra, in which reorientational relaxation is a major contribution, can be also analyzed in the framework of density fluctuations.^{33,34} However, despite of the similar features in $P_2(t)$ and $F_s(\mathbf{k}, t)$, simple

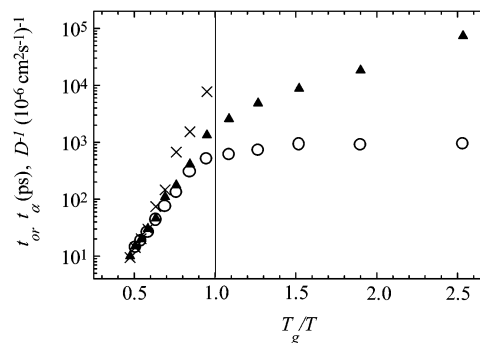


Figure 6. Reorientational relaxation time (circles), inverse of diffusion coefficient (triangles), and structural α relaxation (crosses) of the NO_3^- anions in CKN simulated with the FCM.

inspection of Figure 5 indicates significant differences between them. At low temperature, arrest of the relaxation in $F_s(\mathbf{k}, t)$ is observed whereas $P_2(t)$ still decays (note that the lowest temperature curve in the top panel in Figure 5 is 150 K, whereas it is 350 K in the bottom panel). Thus, whereas the arrest of structural relaxation occurs at temperatures close to T_g , activated hopping processes act as residual mechanisms of reorientational relaxation that relax $P_2(t)$ to zero. This implies decoupling between single-particle and collective dynamics as the glass transition is approached.

To derive relaxation times from the data in Figure 5, the long time decay of these functions have been fitted by a stretched exponential function, $f(t) = A \exp[-(t/\tau)^\beta]$. The fitting procedure is not too straightforward as the resulting set of parameters can be dependent on the actual time range fitted. In addition, similar good fits can be achieved whether the β parameter is kept fixed (for instance, $\beta = 0.8$) at all temperatures or is left as another free adjustable parameter. That implies slightly different values for the best fit relaxation time. We stress that our interest here is the relaxation time in a broad temperature range and, fortunately, the picture drawn in the following is not modified whether slight different protocols of fitting procedure are used.

Figure 6 shows the temperature dependence of the reorientational relaxation time, τ_{or} , the inverse of the diffusion coefficient, D^{-1} , and the structural α relaxation time, τ_α , of CKN simulated with the FCM. They display similar activation energies in the liquid phase, and then different slopes on approaching the glass transition. The values of D and τ_α in Figure 6 are for the NO_3^- anions to compare with τ_{or} , but the same picture would be drawn whether D and τ_α of either the Ca^{2+} or the K^+ ions were considered instead (not shown here). Figure 6 nicely illustrates the coupling between translational diffusion, reorientational relaxation, and structural relaxation in the high-temperature liquid state, and the hierarchy of their decoupling due to the glass transition.

The calculated τ_{or} values are consistent with experimental data, as discussed in the previous section, and the calculated partial $F_s(\mathbf{k}, t)$ shown in Figure 5 also seem reasonable in light of inelastic neutron scattering investigations of CKN.^{9,10} Diffusion coefficients of CKN have not been reported, and it remains to be shown whether the temperature dependence of the diffusion in the simulated system is comparable to the real one. Some previous MD simulations on the temperature dependence of diffusion coefficients concern a temperature range close to T_g , in which the Arrhenius dependence can be replaced by a Vogel–Fucher–Tamman (VFT) dependence or a power law.^{1–6} The prediction of mode-coupling theory (MCT) is that the dynamics changes from diffusion like at a temperature $T_c \approx 1.2T_g$.^{1–6,35} A detailed investigation whether a VFT or other

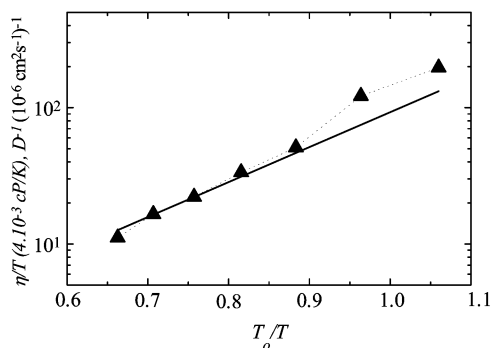


Figure 7. Inverse of the diffusion coefficient (triangles) of the NO_3^- anions in CKN simulated with the FCM. The full line is the experimental η/T data (eq 3),^{36,37} which has been arbitrarily multiplied by a factor of 4×10^3 to match the $D^{-1}(T)$ curve at high temperature. The temperature axis is normalized by the experimental $T_0 = 530$ K.

function is the best one for fitting the present data of CKN would require running other MD simulations in a rather restrict temperature range around T_c to get more data. We stress that our purpose is a study in a much broader temperature range, so we did not attempt to identify T_c of the simulated system. Nevertheless, an estimate of whether the $D(T)$ dependence of the simulated system is physically reasonable can be achieved by comparing with experimental data of viscosity. Detailed investigations on conductivity and viscosity, η , of CKN and several molten nitrates have been reported in a temperature range from the liquid state down to the glass transition.^{36,37} It has been shown that a modified Arrhenius dependence follows^{36,37}

$$\frac{\eta}{T} = \frac{B}{T_0} \exp\left(\frac{qT_0}{T}\right) \quad (3)$$

where $q = 5.9$, and, for CKN, $B = 0.032$ cP, and $T_0 = 530$ K. We could estimate at least whether the temperature dependence of our calculated D in the liquid phase is reasonable by assuming a Stokes–Einstein relation, $D^{-1} \propto (\eta/T)$. Figure 7 shows diffusion coefficients calculated with the FCM for CKN together with the above empirical equation for η/T , arbitrarily scaled in the high-temperature range. The calculated D follow the empirical relation for η/T , the departure of D from eq 3 at $T_0/T \approx 0.9$ being also observed in the experimental η/T data (see Figure 2 in ref 36). As the bending of $\eta(T)$ curves is the feature that characterizes the fragility of a glass-forming liquid, we conclude that the fragility of CKN simulated with the FCM is consistent with the real system. In addition, it has been also shown that a Stokes–Einstein–Debye relation, $\tau_{or} \propto (\eta/T)$, is valid for molten nitrates and CKN at low viscosity, failing as the latter approaches the glass transition.³⁸ Figure 8 shows τ_{or} calculated with the FCM for CKN as a function of the experimental η/T given by eq 3. It is clear from Figure 8 that the simulated system follows the Stokes–Einstein–Debye relation as the real system at high temperature.

Returning to Figure 6, the $\ln(D)$ vs $1/T$ curve indicates that approximate Arrhenius dependence is followed with distinct activation energy in the liquid and in the glassy state, with a bending in the slope between these two regimes at temperatures close to T_g . A similar temperature dependence of D has been also observed in MD simulations of supercooled and glassy ethanol, as the slope of the $D(T)$ curve was smaller in glassy than in liquid ethanol.⁶ In the case of MD simulations of SiO_2 ⁴ and atomic Lennard-Jones systems,³ a downward bending in the $D(T)$ curve has been observed, so that the slope becomes steeper at low temperature, but it should be noted that the

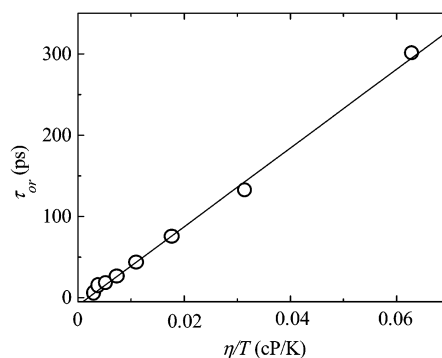


Figure 8. Reorientational relaxation time (circles) of CKN at high-temperature simulated with the FCM as a function of the experimental η/T given by eq 3.^{36,37} The full line is a linear fit to the τ_{or} data.

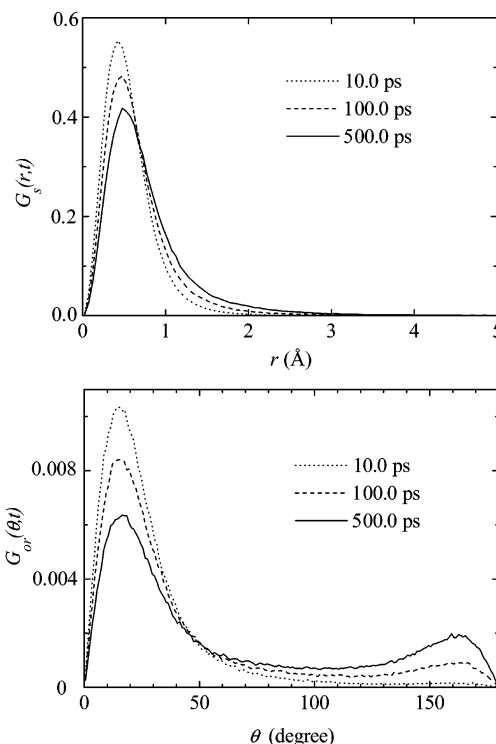


Figure 9. Self-part of the van Hove function $G_s(r,t)$ (top panel) and the orientational analogous $G_{or}(\theta,t)$ (bottom panel), for the NO_3^- anions in CKN simulated with the FCM at 400 K at the indicated times.

temperature range in these studies was above the glass transition. Decoupling between translational and reorientational diffusion, D_t and D_r , respectively, has been identified in NMR investigations of large molecule probes in the glass-forming liquid *o*-terphenyl, OTP.³⁹ At high temperature, the $D_t(T)$ and the $D_r(T)$ curves can be superimposed, whereas distinct slopes are observed as the temperature is decreased below T_c , where $T_c \approx 1.2T_g$. It was observed in ref 39 that the temperature dependence of D_t becomes weaker than D_r on approaching T_g , so that the $D_t(T)$ curve goes above the $D_r(T)$ curve. This is in contrast with the present results on CKN shown in Figure 6, in which the inverse of diffusion coefficients are given. This distinct behavior of the translational/reorientational decoupling in CKN and in OTP could be assigned to the very different size of the molecules. Reorientational jumps of large probe molecules should become very hindered in supercooled OTP in comparison to the reorientation of a relatively small NO_3^- anion in CKN. This proposal is strengthened by previous MD simulations of simple models of diatomic Lennard-Jones molecules,⁴⁰ where, in line with the present results on CKN, the slope of the $D_r(T)$

curve becomes weaker than the $D_i(T)$ curve on cooling the system.

The ionic dynamics in CKN simulated with the FCM has been discussed in previous publications by using several time correlation functions.^{17,18} Activated hopping processes are usually detected in MD simulations by the self-part of the van Hove correlation function, $G_s(r, t) = \langle \delta[\mathbf{r} + \mathbf{r}_i(0) - \mathbf{r}_i(t)] \rangle$. In the case of hopping processes occurring at low temperatures, a secondary peak in $G_s(r, t)$ is observed at large distance at long time. An orientational analogous to $G_s(r, t)$ can be also defined, $G^{or}(\theta, t) = \langle \delta[\theta_i - \theta_i(t)] \rangle$, where $\theta_i(t)$ is the angle made by an unitary vector on the C_3 axis of a given NO_3^- anion at time t in relation to its value at $t = 0$. Figure 9 shows $G_s(r, t)$ and $G^{or}(\theta, t)$ of the NO_3^- anions calculated with the FCM for CKN at $T = 400$ K. It is clear from Figure 9 that a secondary maximum is found for $G^{or}(\theta, t)$ but not for $G_s(r, t)$. Therefore, at a temperature close to the estimate $T_g \approx 380$ K of the simulated system, reorientational hopping is seen in the $G^{or}(\theta, t)$ but translational hopping is no yet seen in $G_s(r, t)$. This finding strengthens the picture that hopping processes are more effective in the single particle reorientational dynamics than in the translational dynamics in CKN, which in turns gives the weaker temperature of τ_{or} than D as the glassy state is approached.

IV. Concluding Remarks

Molecular dynamics simulations of the archetypical fragile glass-forming liquid $\text{Ca}_{0.4}\text{K}_{0.6}(\text{NO}_3)_{1.4}$, CKN, have been done with the polarizable fluctuating charge model, FCM, for the NO_3^- anion. The broad temperature range investigated (800–150 K) encompasses the well-equilibrated liquid state down to a deeply cooled glassy state. By running some short MD simulations of liquid CKN at high temperature, it was shown that the recently proposed method of a truncated and shifted Coulomb potential¹⁹ gives results similar to those from simulations with the well-established Ewald sum method of handling the long-range interactions.

Comparisons between simulated and experimental data indicate that the dynamics of the real system is well captured by the FCM for CKN. It has been shown that the previously observed¹⁷ increase in ionic mobility in CKN when polarization effects are included in the simulations indeed implies a glass transition temperature T_g in closer agreement with the experimental value than the nonpolarizable model counterpart. The temperature dependence of single-particle translational and reorientational dynamics and the structural relaxation has been investigated. The main upshot of the present simulations was that τ_{or} , D^{-1} , and τ_α display the same activation energy at the high-temperature liquid state, but they decouple as the glass transition is approached. Whereas the $D^{-1}(T)$ and the $\tau_{or}(T)$ curves can be superimposed at high temperature, the latter falls below the former as T_g is approached, so that the slope of the $\tau_{or}(T)$ curve, and therefore its activation energy, are smaller than the $D^{-1}(T)$ at low temperature. It is then suggested that hopping processes are more effective in the relaxation of the reorientational than the translational dynamics, which is corroborated by the corresponding van Hove correlation functions. On the other hand, the structural relaxation time τ_α displays a divergent behavior as T_g is approached prior to the structural arrest.

The occurrence of dynamical heterogeneity in CKN has been proposed on the basis of NMR investigations of reorientational dynamics of the NO_3^- anions.^{12,13} It has been suggested that populations of fast and slow reorientating anions coexist in the supercooled liquid. In the last years, MD simulations have been

intensively used in studying dynamical heterogeneity mainly in simple atomic Lennard-Jones model systems, in which of course only translational heterogeneity is of concern.^{41,42} Studying simultaneous translational and reorientational heterogeneity in CKN would be of interest. The present results on coupling (and further decoupling) between translational and reorientational dynamics in the simulated CKN suggest the interesting question whether there is any correlation between the islands of fast or slow dynamics of each of the degrees of freedom. The estimated T_g close to the experimental one is an advantage of the FCM for CKN, because it would be desirable to perform the simulations with a model that satisfactorily reproduces the dynamics of the real system at a given temperature. The study of dynamical heterogeneity in CKN simulated with the FCM is now in progress.

Acknowledgment. The computation facilities of the LCCA at the Universidade de São Paulo is acknowledged. I am indebted to FAPESP and CNPq for financial support.

References and Notes

- (1) Barrat, J.-L.; Klein, M. L. *Annu. Rev. Phys. Chem.* **1991**, *42*, 23.
- (2) Kob, W. *J. Phys.: Condens. Matter* **1999**, *11*, R85.
- (3) Kob, W.; Andersen, H. C. *Phys. Rev. E* **1995**, *52*, 4134.
- (4) Horbach, J.; Kob, W.; Binder, K. *Philos. Mag. B* **1998**, *77*, 297.
- (5) Lewis, L. J.; Wahnström, G. *Phys. Rev. E* **1994**, *50*, 3865.
- (6) González, M. A.; Enciso, E.; Bermejo, F. J.; Bée, M. *Phys. Rev. B* **2000**, *61*, 6654.
- (7) Angell, C. A. *Science* **1995**, *267*, 1924.
- (8) Angell, C. A. *J. Phys.: Condens. Matter* **2000**, *12*, 6463.
- (9) Mezei, F. *Ber. Bunsen-Ges. Phys. Chem.* **1991**, *95*, 1118.
- (10) Tengroth, C.; Swenson, J.; Isopo, A.; Börjesson, L. *Phys. Rev. B* **2001**, *64*, 224207.
- (11) Jacobsson, P.; Börjesson, L.; Hassan, A. K.; Torell, L. M. *J. Non-Cryst. Solids* **1994**, *172–174*, 161.
- (12) Sen, S.; Stebbins, J. F. *Phys. Rev. Lett.* **1997**, *78*, 3495.
- (13) Sen, S.; Stebbins, J. F. *Phys. Rev.* **1998**, *58*, 8379.
- (14) Signorini, G. F.; Barrat, J.-L.; Klein, M. L. *J. Chem. Phys.* **1990**, *92*, 1294.
- (15) Ribeiro, M. C. C. *Phys. Rev. B* **2000**, *61*, 3297.
- (16) Ribeiro, M. C. C.; Almeida, L. C. J. *J. Chem. Phys.* **2000**, *113*, 4722.
- (17) Ribeiro, M. C. C. *Phys. Rev. B* **2001**, *63*, 094205.
- (18) Ribeiro, M. C. C. *J. Chem. Phys.* **2001**, *114*, 6714.
- (19) Wolf, D.; Koblinski, P.; Phillpot, S. R.; Eggebrecht, J. *J. Chem. Phys.* **1999**, *110*, 8254.
- (20) Allen, M. P.; Tildesley, D. J. *Computer Simulation of Liquids*; Oxford University Press: Clarendon Park, U.K., 1987.
- (21) Demontis, P.; Spanu, S.; Suffritti, G. B. *J. Chem. Phys.* **2001**, *114*, 7980.
- (22) Zahn, D.; Schilling, B.; Kast, S. M. *J. Phys. Chem. B* **2002**, *106*, 10725.
- (23) Rappé, A. K.; Goddard, W. A., III. *J. Phys. Chem.* **1991**, *95*, 3358.
- (24) Rick, S. W.; Stuart, S. J.; Berne, B. J. *J. Chem. Phys.* **1994**, *101*, 6141.
- (25) Berendsen, H. J. C.; Postma, J. P. M.; van Gusteren, W. F.; DiNola, A.; Haak, J. R. *J. Chem. Phys.* **1984**, *81*, 3684.
- (26) Kartini, E.; Collins, M. F.; Collier, B.; Mezei, F.; Svensson, E. C. *Can. J. Phys.* **1995**, *73*, 748.
- (27) Vollmayr, K.; Kob, W.; Binder, K. *J. Chem. Phys.* **1996**, *105*, 4714.
- (28) Buchholz, J.; Paul, W.; Varnik, F.; Binder, K. *J. Chem. Phys.* **2002**, *117*, 7364.
- (29) Horbach, J.; Kob, W.; Binder, K.; Angell, C. A. *Phys. Rev. E* **1996**, *54*, R5897.
- (30) Rothschild, W. G. *Dynamics of Molecular Liquids*; Wiley: New York, 1984.
- (31) Kirillov, S. A. *J. Mol. Liq.* **1998**, *76*, 35.
- (32) Ricci, M.; Foggi, P.; Righini, R.; Torre, R. *J. Chem. Phys.* **1993**, *98*, 4892.
- (33) Li, G.; Du, W. M.; Chen, X. K.; Cummins, H. Z. *Phys. Rev. A* **1992**, *45*, 3867.
- (34) Rössler, E.; Sokolov, A. P.; Kisliuk, A.; Quitmann, D. *Phys. Rev. B* **1994**, *49*, 14967.
- (35) Sokolov, A. P. *Endeavour* **1997**, *21*, 109.
- (36) Voronel, A.; Veliyulin, E.; Grande, T.; Øye, H. A. *J. Phys.: Condens. Matter* **1997**, *9*, L247.

(37) Veliyulin, E.; Shasha, E.; Voronel, A.; Machavariani, V. Sh.; Seifer, Sh.; Rosenberg, Y.; Shumsky, M. G. *J. Phys.: Condens. Matter* **1999**, *11*, 8773.

(38) Kisiuk, A.; Loheider, S.; Sokolov, A. P.; Soltwisch, M.; Quitmann, D.; Shasha, E.; Voronel, A. *Phys. Rev. B* **1995**, *52*, R13083.

(39) Chang, I.; Fujara, F.; Geil, B.; Heuberger, G.; Mangel, T.; Sillescu, H. *J. Non-Cryst. Solids* **1994**, *172–174*, 248.

(40) Kämmerer, S.; Kob, W.; Schilling, R. *Phys. Rev. E* **1997**, *56*, 5450.

(41) Richert, R. *J. Phys.: Condens. Matter* **2002**, *14*, R703.

(42) Glotzer, S. *J. Non-Cryst. Solids* **2000**, *274*, 342.